March 24, 2021

The Degree of Polymerization and Sulfation Patterns in Heparan Sulfate are Critical Determinants of Cytomegalovirus Entry into Host Cells

Mohammad H. Hasan[1#], Dipanwita Mitra[1#], Rinkuben C. Parmar[1], Lauren A. Fassero, Quntao Liang[2,6], Hong Qiu[3], Vaibhav Tiwari[4], Joshua S. Sharp[2], Lianchun Wang[5] and Ritesh Tandon[1]*

[1]Department of Microbiology and Immunology, University of Mississippi Medical Center, 2500 North State Street, Jackson, MS 39216, USA. [2]Department of Biomolecular Sciences, School of Pharmacy, University of Mississippi, Oxford, MS 38677, USA. [3]Complex Carbohydrate Research Center, University of Georgia, Athens, GA 30602. [4]Department of Microbiology and Immunology, Midwestern University, Downers Grove, IL, 60515, USA. [5]Department of Molecular Pharmacology and Physiology, University of South Florida, Tampa, FL 33612, USA. [6]College of Biological Science and Engineering, University of Fuzhou, Fujian, 350108, China.

#Equal contributions

***Corresponding Author:** Ritesh Tandon

Phone: 601-984-1705, Fax: 601-984-1708, Email: rtandon@umc.edu

Keywords: CMV, herpesviruses, heparan sulfate, sulfation

Running title: HS as CMV attachment receptors

ABSTRACT

Several enveloped viruses, including herpesviruses attach to host cells by initially interacting with cell surface heparan sulfate (HS) proteoglycans followed by specific coreceptor engagement which culminates in virus-host membrane fusion and virus entry. Interfering with HS-herpesvirus interactions has long been known to result in significant reduction in virus infectivity indicating that HS play important roles in initiating virus entry. In this study, we provide a series of evidence to prove that specific sulfations as well as the degree of polymerization (*dp*) of HS govern human cytomegalovirus (CMV) binding and infection. First, purified CMV extracellular virions preferentially bind to sulfated longer chain HS on a glycoarray compared to a variety of unsulfated glycosaminoglycans including unsulfated shorter chain HS. Second, the fraction of glycosaminoglycans (GAG) displaying higher *dp* and sulfation has a larger impact on CMV titers compared to other fractions. Third, cell lines deficient in specific glucosaminyl sulfotransferases produce significantly reduced CMV titers compared to wild-type cells and virus entry is compromised in these mutant cells. Finally, cells pretreated with a peptide that specifically binds sulfated-HS produce significantly reduced virus titers compared to the control peptide treated cells. Taken together, these results highlight the significance of HS chain length and sulfation patterns in CMV attachment and infectivity.

IMPORTANCE

Heparan sulfate (HS) is a linear polysaccharide found in all animal tissues. It binds to a variety of protein ligands, including cytokines, chemokines, growth factors and morphogens and regulates a wide range of biological activities, including developmental processes, angiogenesis, blood coagulation, and tumor metastasis. The molecular diversity in HS chains generates unique binding sites for specific ligands and can offer preferential binding for a specific virus over other viruses or cellular ligands. In the current study human cytomegalovirus (CMV) was found to bind preferentially to uniquely sulfated and polymerized HS. The HS mimics designed with these properties inhibited CMV infection. The results were corroborated by parallel studies in mutant mouse cells as well as using peptide inhibition. Combined together, the data suggests that CMV preferentially attaches to uniquely modified HS and thus this virus-host interaction is amenable to targeting by specifically designed HS mimics or peptides.

INTRODUCTION

The heparan sulfate (HS) proteoglycans are present on most cell types and function as cellular attachment receptors for medically important viruses, including human immunodeficiency virus (HIV), hepatitis-C virus (HCV), human papillomavirus (HPV), Dengue virus (DENV) and the recently emerged SARS-CoV-2 (1, 2) (3-6). In addition, virtually all human herpesviruses, with the possible exception of Epstein Barr virus, use HS as an initial co-receptor for entry (7). The interaction between cell surface HS and virus envelope is the initial event in the complex process of virus entry. A successful virus entry involves downstream co-receptor interactions ultimately leading to fusion between the virus envelope and the cell membrane (8).

Herpesviruses and several other enveloped viruses enter the host cells using two distinct pathways: 1) A pH-independent pathway which involves the fusion of the virus envelope with the plasma membrane; and 2) A pH-dependent pathway that involves endocytosis of the virus particle (9). In cells, where binding of virus to cell surface receptors induces endocytosis, the usual consequence is the acidification of the endosome, which ultimately triggers fusion between the virus envelope and endosomal membrane (7). Interestingly, human cytomegalovirus (HCMV) entry follows direct fusion at the cell surface in fibroblasts, while entry into other relevant cell types, such as endothelial cells, follows an endocytic route (10, 11). Different virus glycoprotein complexes are involved in each case; however, HS functions as the primary attachment receptor. Moreover, the presence of HS receptors are well documented in endosomal membranes and HS receptors likely play roles in intracellular virus trafficking (12-15).

The herpesvirus envelope is a lipid bilayer derived from host cell membranes in which most cellular proteins have been displaced by viral membrane proteins. For HCMV, at least twenty three different viral glycoproteins have been found to be associated with purified virion preparations (16). For most herpesviruses, the conserved glycoprotein B (gB) is required for virus entry and binds to cell surface molecules, including HS, which is present not only as a constituent of cell surface proteoglycans but also as a component of the extracellular matrix and basement membranes in organized tissues (7, 17). HCMV gB binds to HS resulting in virus attachment (18) similar to its counterparts in herpes simplex virus (HSV)-1 (17, 19) and varicella-zoster virus (VZV) (20). Subsequently, HCMV gB binds to cellular protein receptors such as EGFR (21), PDGFα (22), and integrins (23, 24), which culminates in virus entry. Treatment of cells with soluble form of gB inhibits HCMV entry (25). HCMV binding and infection are reduced by soluble heparin and HS, as well as in cells treated with heparinases or those unable to produce HS (26). A better structural understanding of these inhibitions will pave the way to design effective antivirals that are highly specific as well as more effective.

The synthesis of HS is a complex process involving multiple specialized enzymes and is initiated from a tetrasaccharide (GlcA-Gal-Gal-Xyl) that is attached to the core protein (Fig. 1A). HS polymerase is responsible for building the polysaccharide backbone with a repeating unit of -GlcA-GlcNAc- (Fig. 1B). The backbone is then modified by N-deacetylase/N-sulfotransferase (NDST) responsible for N-deacetylation and N-sulfation of selected glucosamine residues, C5-epimerase responsible for epimerization of selected glucuronic moieties to iduronic acid, 2-*O*-sulfotransferase

(Hs2st; 2-*O*-ST) responsible for 2-*O*-sulfation of selected iduronic acid residues, 6-*O*-sulfotransferase (H6st; 6-*O*-ST) for 6-*O*-sulfation and finally (but rarely) 3-*O*-sulfotransferases (Hs3st; 3-*O*-ST) responsible for 3-*O*-sulfation (27, 28). The substrate specificities of these biosynthetic enzymes dictate the structures of HS products, including sulfation levels, the contents of L-iduronic acid (IdoA) units and the size of the polysaccharides (27). The location of the sulfo groups and IdoA in turn play a crucial role in determining the binding and functions of HS.

In the current study, we investigated the impact of specific sulfations as well as degree of polymerization in terms of numbers of monosaccharide units (*dp*) in HS chain on both human and mouse CMV infection and binding. Purified CMV extracellular virions preferentially bound strongly to the longer sulfated HS chains but not to the shorter unsulfated HS chains on a glycoarray. Glycosaminoglycans of different *dp* were derivatized from enoxaparin (a low molecular weight heparin) and tested for their ability to inhibit CMV infection in cell culture. The results show that longer glycan chains are more efficient at reducing CMV titers in cells compared to shorter chain glycans. Also, the cell lines defective in expression of various sulfotransferases showed significantly reduced CMV entry and replication. Finally, cells pre-treated with peptides that bind HS and 3-*O*-S HS (29-32) significantly reduced HCMV titers compared to a control peptide. Overall, these results indicate that CMV binding to cell surface glycans is dependent on branch length and sulfation pattern of HS.

MATERIALS AND METHODS

Preparation of glycosaminoglycans (GAGs) oligosaccharides. Glycosaminoglycans of different *dp* were fractionated from enoxaparin (a low molecular weight heparin) by Bio-Gel P-10 chromatography as previously described (33). Briefly, 15 mg/mL enoxaparin sodium derived from porcine intestinal mucosa (Sanofi-Aventis U.S., Bridgewater, NJ) was applied to a Bio-Gel P-10 column (2.5X120 cm, Bio-Rad, Hercules CA) and eluted with 0.2 M NH_4HCO3 at a flow rate of 14 ml/h. Elution of oligosaccharides was monitored by absorbance at 232 nm. NH_4HCO3 was removed by heating in oven at 50 °C for 24 h.

Preparation of the 6-*O* desulfated Arixtra with MTSTFA. A detailed procedure on the preparation of 6-*O* desulfated Arixtra was published previously (34). Briefly, 4 mg of Arixtra was added to 10 volumes (w/w) of N-Methy-N-(trimethylsilyl)-trifluoroacetamide (MTSTFA, Sigma, ≥98.5%) and 100 volumes (v/w) of pyridine. The mixture was heated at 100 ℃ for 30 min, then quickly cooled in an ice-bath, followed by extensive dialysis and freeze-drying. The sample was resuspended in 50% acetonitrile/water at a concentration of 30 µM for later LC-MS/MS analysis.

LC-MS/MS analysis. The 6-*O*-desulfated Arixtra (30 µM) was analyzed on a Thermo Orbitrap Fusion Tribrid (Thermo Fisher Scientific) coupled with an Ultimate 3000 Nano LC system (Dionex) using direct infusion. The flow rate was set to 1 µl/min. Mobile-phase was 50% acetonitrile. Nanoelectrospray voltage was set to 2.0 kV in negative ion mode. Full MS scan range was set to 200-2000 m/z at a resolution of 60,000, RF lens

was 6%, and the automatic gain control (AGC) target was set to 2.0 × 105. For the MS/MS scans, the resolution was set to 50,000, the precursor isolation width was 3 m/z units, and ions were fragmented by collision-induced dissociation (CID) at a normalized collision energy of 80%.

Cells. Mouse embryonic fibroblasts (MEF) and human foreskin fibroblasts (HFF) were cultured in Dulbecco's modified Eagle's medium (DMEM, Cellgro, Manassas, VA) containing 4.5 g/ml glucose, 10% fetal bovine serum (SAFC, Lenexa, KS), 1 mM sodium pyruvate, 2 mM L-glutamine, and 100 U/ml penicillin-streptomycin (Cellgro, Manassas, VA) at 37 °C with 5% CO2. Mouse lung endothelial cells (WT, H3st1$^{-/-}$, H3st4$^{-/-}$, H3st1/4-double-knockout, H6st1$^{-/-}$, H6st2$^{-/-}$, and H6st1/2 double-knockout) were obtained from Wang laboratory at University of South Florida and maintained as described earlier (35).

Virus. MCMV (strain K181) was grown in MEF cells, while HCMV (Towne strain) was grown on HFF cells. Virus stock was prepared in 3X autoclaved milk, sonicated 3 times and stored at −80 °C. 3X autoclaved milk is prepared from Carnation (Nestle) instant nonfat dry milk powder. 10% milk was prepared in nano pure water, pH was adjusted to 7.0 and was autoclaved for 3 times. During infection, media was removed from the wells of cell culture plates and appropriately diluted virus stock was absorbed onto the cells in DMEM without serum. Cells were incubated for 1 hour with gentle shaking every 10 mins followed by washing 3X with PBS. Fresh complete medium was added and cells

were incubated until the end point. For extracellular virus (ECV) purification, HFF were seeded in roller bottles, grown to confluency and infected with HCMV (Towne strain) at MOI of 0.01. Two days after 100% cytopathic effect was observed, infected cell medium was collected and centrifuged at low speed to pellet cellular debris, and the supernatant was transferred to new tubes and centrifuged at 20,000 g for 1 hour to pellet the ECV. This ECV pellet was re-suspended in phosphate buffer, sonicated to eliminate any aggregates, loaded over 15-50% continuous sucrose gradients and centrifuged in a SW-41 rotor at 39,000 RPM for 20 min. ECV bands were visualized in incandescent light and harvested by puncturing the sides of the centrifuge tubes. These bands were washed once with phosphate buffer, spun again and the final pellet resuspended in low salt phosphate buffer. An aliquot of the sample was used for assessment of initial quality of ECV by negative staining and transmission electron microscopy. Purified ECV were shipped on ice to Z biotech (Aurora, CO) for glycoarray binding analysis.

Cell viability assay. HFF cells plated in 12 well tissue culture plates were grown to confluency and pretreated for 1h with 10 µM concentration of candidate HS and then infected with HCMV (Towne strain) at a multiplicity of infection (MOI) of 3.0 or mock-infected in the presence of candidate HS . Five hundred µl of fresh complete medium containing HS was added to the wells on day 3 and day 6. At the designated time points, media was removed and cells were harvested by trypsinization. Cell viability was determined using trypan blue exclusion on TC20 automated cell counter (BioRad Laboratories, Hercules, CA) following manufacturer's protocol.

188 **Virus titers.** Infected or mock-infected samples were harvested within the medium at
189 the designated end points and stored at −80 °C before titration. In some experiments,
190 media and cells were separated by low-speed (< 1000 × g) centrifugation and viral
191 loads in supernatant and cells were quantified by titering on wild-type cells. Titers were
192 performed as described earlier (36) with some modifications. In brief, monolayers of
193 fibroblasts grown in 12 well plates and serial dilutions of sonicated samples were
194 absorbed onto them for 1 h, followed by 3X washing with PBS. Carboxymethylcellulose
195 (CMC) (Catalog No. 217274, EMD Millipore Corp., Billerica, MA) overlay with complete
196 DMEM media (1-part autoclaved CMC and 3 parts media) was added and cells were
197 incubated for 5 days. At the end point, overlay was removed and cells were washed 2X
198 with PBS. Infected monolayers were fixed in 100% methanol for 7 min, washed once
199 with PBS and stained with 1% crystal violet (Catalog No. C581-25, Fisher Chemicals,
200 Fair Lawn, NJ) for 15 min. Plates were finally washed with tap water, air dried and
201 plaques with clear zone were quantified.

202

203 **Immunoblots.** Mouse lung endothelial cells (WT, H3st1$^{-/-}$, H3st4$^{-/-}$, H3st1/4-double-
204 knockout, H6st1$^{-/-}$, H6st2$^{-/-}$, and H6st1/2 double-knockout) were infected with MCMV
205 (K181 strain) and an MOI of 3.0 and the whole cell lysates were harvested at 2 hours
206 post infection for analysis. The blot was probed with anti -IE1 antibody (catalog no. HR-
207 MCMV-12, Center for Proteomics, University of Rijeka, Croatia) and HRP-conjugated
208 goat anti mouse antibody (PI131444, Invitrogen) was used as the secondary antibody.

209

Glycoarrays. A dilution series of purified HCMV virions were incubated on two different custom glycoarrays (Table 1 and Table 2, Z-Biotech) using established protocols (37) and the arrays were analyzed to assess specific virus binding. Briefly, 10^5 to 10^8 pfu/ml of purified virions were incubated for an hour on glycoarrays containing six replicates of each glycosaminoglycan. After incubation, staining with primary antibody (mouse anti gB (clone 2F12, Virusys Inc, Taneytown, MD) was done at 100 µg/ml and secondary antibody (Goat anti mouse IgG AlexaFlour555) was done at 1µg/ml. Maximum strength fluorescent signal was obtained for 10^8 pfu/ml concentration of the virus, therefore, only this concentration is represented in the final data obtained for plotting the graphs.

Treatment of HFF cells with anti-HS and anti-3-*O*-S HS peptides. HFF cells were pre-treated with the phage display derived peptides (1 mg/ml) generated against wild-type HS (LRSRTKIIRIRH), and 3-*O*-S HS (MPRRRRIRRRQK) (29) that bind specifically to HS and 3-*O*-S HS respectively, or left mock treated for 4 hours before the cells were infected with β-galactosidase expressing CMV (ATCC) for 9 days. β-Galactosidase assay was performed using X-gal (Sigma). The effect of entry- blocking activity of peptide was examined by counting number of virus foci.

Statistics: Student's t-tests were conducted in Graphpad Prism comparing the means of different groups (GraphPad Prism version 8.0.0, GraphPad Software, San Diego, California USA, www.graphpad.com). Standard error of mean was plotted as error bars. A p value of <0.05 was considered significant.

RESULTS

Purified HCMV extracellular virions preferentially bind to sulfated glycosaminoglycans with increased degree of polymerization.

First, we sought to establish the category of GAG that preferentially binds to purified HCMV virions. HCMV extracellular virions were purified as described above and incubated with custom glycoarrays containing increasing molecular weight species of hyaluronic acid, heparin, chondroitin sulfate, and dermatan sulfate (Table 1). HCMV binding to non-sulfated hyaluronic acid (HA10 to HA20 and HA93 polymer) was negligent but significant binding to all heparin species was detected with a trend of increased binding to heparins as their *dp* increased (Fig. 2). HCMV also bound to large size chondroitin sulfate D (GAG28, *dp20*), and dermatan sulfate oligosaccharides (GAG32- GAG34, *dp16-dp20*) but not to chondroitin sulfate AC (GAG17- GAG22). It is important to note that while the chondroitin sulfate A (CS-A) is sulfated at C4 of the GalNAc, and the chondroitin sulfate C (CS-C) is sulfated at the C6 of the GalNAc only, the chondroitin sulfate D is sulfated at C2 of the glucuronic acid as well as the C6 of the GalNAc sugar and hence has double the amount of sulfation compared to CS-A and CS-C. Dermatan sulfate (DS), formerly referred to as CS-B, is formed from the polymer backbone of chondroitin sulfate by the action of chondroitin-glucuronate C5 epimerase, which epimerizes individual d-glucuronic acid residues to l-iduronic acid. The binding affinity to DS was also size-dependent increasing from GAG32- GAG34 (*dp16- dp20*). Heparin (*dp30*) was the best HCMV binder in this assay. The virus preparation does not contain streptavidin label and thus positive control 1 (PC1) serves as a negative rather than a positive control.

On a second HS specific array (Table 2), HCMV showed strong binding to the HS with longer monosaccharide chains (HS007 to HS024) and minimal binding to unsulfated glycans (HS001-HS006) (Fig. 3). The maximum binding was observed for HS014, HS015 and HS016, which are all 6-*O*-S 9-mers with moderate amount of sulfation (1.3-1.8 sulfate group per disaccharide). Also, significant amount of binding was observed for 2-*O*-S (HS17-HS19), 6-*O*-S/2-*O*-S (HS20-22) and 2-*O*-S/6-*O*-S/3-*O*-S (HS23-24) HS that had high amount of sulfation (1.3-2.7 sulfate group per disaccharide) and 6-8 disaccharides per chain. Overall the data from these experiments indicate that the *dp* of HS as well as sulfation is important for HCMV binding.

The degree of polymerization of GAG chains impacts CMV infectivity.

Glycosaminoglycans of different *dp* were fractionated from enoxaparin (a low molecular weight heparin). All of these GAGs are based on a HS backbone and differ in either *dp* or degree/place of sulfation or both (Fig. 4, S1). These GAGs, along with heparin and Arixtra (fondaparinux sodium), were first screened in a GFP-based preliminary virus focus reduction assay using GFP tagged HCMV (Towne strain). The viral GFP expression was most efficiently reduced by heparin salt (PIHSS; Heparin sodium salt from porcine intestinal mucosa) whereas Arixtra, 6-*O*-desulfated Arixtra and enoxaparin had little to no impact on GFP expression (Fig. 4). In general, enoxaparin derived GAGs with higher *dp* were more efficient in reducing viral GFP compared to low *dp* derivatives. To follow up on this primary GFP based screening, we performed viral titer assay using HCMV (Towne strain) that measures total virus yields at 5 days post-infection. Most reduction in viral titers was observed for heparin (PIHSS) followed by enoxaparin

278 derivative with >20 *dp* (Fig. 5A). Plotting of viral titer reduction as a function of *dp*
279 revealed a general trend where higher *dp* derivatives lead to higher reduction in viral
280 titers (Fig. 5B). Thus, this experiment indicated that longer HS chains are more efficient
281 at reducing HCMV titers in cells. To investigate whether this inhibitory effect was due to
282 an increase in the number of HCMV binding sites per chain of longer chain GAGs
283 towards virus particles, the experiments were repeated at 0.05 g/L concentrations of
284 GAGs instead of the previously used molar equivalent concentrations (Fig. 6A). As
285 micromolar concentration (10 µM) of GAGs is based on number of molecules provided,
286 GAGs consisting of longer chain will have more potential binding sites for virus than
287 those of shorter chains. The other concentration (0.05 g/L) is based on weight; thus this
288 concentration normalizes the number of potential virus binding sites for GAGs
289 consisting of both long and short chains. Interestingly, similar trend of inhibitory results
290 leaning towards efficacy of higher *dp* against HCMV infection were obtained at 0.05 g/L
291 indicating that this effect is not merely due to a higher number of potential independent
292 binding sites in the longer GAG chains and instead involves a difference in the
293 molecular interaction between HCMV and the longer GAG chains. A line graph for each
294 concentration of GAGs was generated that demonstrates the relationship of viral titer
295 and degree of polymerization (Fig. 6B). Although GAG treatment is not known to induce
296 cell death, to rule out that these effects on virus titers could be attributed to the health of
297 cells, we performed cell viability assays in both uninfected and infected settings. Cell
298 viability was not affected at the treated concentrations of any of our test GAGs (Fig. 7A).
299 Moreover, heparin (PIHSS) and enoxaparin derivatives (*dp* 12 or greater) efficiently
300 protected cells from virus induced lytic death (Fig. 7B). These results corroborate the

results of our glycoarray experiments that showed that GAG with higher *dp* have higher CMV binding compared to GAG with lower *dp* (Fig. 3).

Cell lines defective in expression of specific sulfation enzymes have reduced CMV titers and reduced virus entry.

Due to species specificity of HCMV, animal models are frequently used to study CMV pathogenesis (38, 39). Studies of murine CMV (MCMV) infections of mice have served a major role as a model of CMV biology and pathogenesis (40). Lung endothelial cell lines from adult mice were mutated for specific sulfotransferase enzymes by a CRISPR-Cas9 based gene editing system (35, 41, 42). Since previous studies showed that 3-*O*-S HS is important for HCMV entry in human iris stromal cells (43), we analyzed virus replication in Hs3st1 and Hs3st4 (Glucosaminyl 3-*O*-sulfotransferase 1 and 4, respectively) knockout cell lines as well as the Hs3st1/4 double knockout cell line. At high (5.0) as well as low (0.01) multiplicity of infection (MOI), MCMV growth was significantly reduced in the single Hs3st1 and Hs3st4 knockouts as well as in the double Hs3st1/4 knockouts, indicating that 3-*O*-sulfation of HS is important for HCMV infection (Fig. 8). Further, we probed whether virus entry is impacted in the cells knocked out for different combinations of these sulfotransferases. Expression of viral immediate early protein (IE1) has been used as a surrogate for virus entry since it's one of the earliest events after a successful virus entry (44-46). Results of an immunoblot probing for IE1 show that virus entry is significantly impacted in H3st1$^{-/-}$, H3st4$^{-/-}$, H3st1/4-double-knockout, H6st1$^{-/-}$, H6st2$^{-/-}$, and H6st1/2 double-knockout cells, compared to the wild-

type cells (Fig. 9A and B). The H6st1$^{-/-}$, H6st2$^{-/-}$ and H3st4$^{-/-}$ mutants showed the most impact on MCMV entry.

Peptides generated against HS and 3-*O*-S HS block HCMV infection.

In order to examine the effect of sulfated HS on HCMV infection, we utilized phage display derived anti-HS and anti-3-*O*-S HS peptide (29). These peptides bind specifically to cellular HS and 3-*O*-S HS respectively, and have been shown to block binding of HSV-1. The HFF cells were pre-treated with either the anti-HS peptide or the anti-3-*O*-S HS peptide and the mock-treated cells were used as control. As indicated in Fig. 10, the anti-3-*O*-S HS peptide treatment resulted in a significant reduction of HCMV foci in HFF cells compared to an anti-HS peptide or the mock-treated cells. The fact that anti-3-*O*-S HS peptide was much more effective at reducing HCMV foci compared to an anti-HS peptide indicates that this effect is governed by HS structure and not only by the peptide charge.

DISCUSSION

In this study, we utilized multiple approaches, including glycoarray binding analysis, HS mimics, HS mutant cell lines, and anti-HS/3-*O*-S HS peptides to demonstrate that specifically sulfated HS with higher degree of polymerization affect CMV infection and binding. The results significantly advance the age-old knowledge of HS binding to herpesviruses by illustrating the importance of HS structural modifications in CMV binding and infection. We first screened several sulfated or unsulfated GAGs with

complex sugar structure to investigate which GAGs are more efficient at binding to HCMV virions. This glycoarray analysis indicated that HCMV bound heparins with strong affinity and showed increased affinity for longer chain length heparins (Fig. 2). To further investigate this binding, we utilized another glycoarray consisting of HS of varied polymerization and sulfation levels. The results from this glycoarray indicated that HCMV binds strongly with HS having both longer monosaccharide chain and a moderate level of sulfation (Fig. 3). Thus, sulfated HS with more complex branches and sulfation patterns preferentially bind to HCMV. Next, we fractioned HS by length (*dp* 2-20) from enoxaparin and tested their ability to inhibit HCMV growth in cell culture by competing with HCMV binding. The GFP tagged HCMV was used and the number of GFP+ foci was quantified in the presence of increasing HS chain length. Amounts of viral GFP was more effectively reduced when cells were pretreated and maintained with GAGs having a higher *dp* (Fig. 4). This assay served as a surrogate for a virus entry assay since the GFP is independently expressed from an early promoter in the virus genome (47). For a deeper understanding of this reduction, we performed a similar experiment where HCMV Towne strain was used and viral load was quantified at 5 days post-infection. Significant reduction in virus titers was observed in samples treated with higher *dp* of GAG but not with lower *dp* corroborating the results from glycoarray experiments that chain length of GAG is an important factor in determining HCMV binding. Also, this effect was not due to a simple increase in the number of potential HCMV binding sites per mole of GAG, as evidenced by similar trend of inhibition obtained when treating cells with equivalent μM or g/L concentrations of GAGs. Treatment of cells with these GAGs did not affect cell viability for the duration of

368 treatment (Fig. 7A) confirming that the observed reduction in virus titer was not due to
369 the cell death. Moreover, cells pretreated and maintained with GAGs of longer *dp*
370 resisted infection induced cell death at late time post-infection (Fig. 7B). We also tested
371 the impact of specific HS sulfation mutants on MCMV infection. As 3-*O* sulfation has
372 been reported to be critical for herpesvirus entry (43, 48), we tested MCMV growth in
373 Hs3st1, Hs3st4 and dual Hs3st1/4 knockout cells. For both high and low MOI, virus titer
374 was significantly reduced in Hs3st1, Hs3st4 and dual Hs3st1/4 knockout cells (Fig. 8).
375 Although the differences were statistically significant, we did not see a robust inhibition
376 of virus titers in these assays and also the double knockout had somewhat less
377 reduction overall. This could largely be explained by the possible presence of additional
378 isoforms of Hs3st1 and Hs3st4 in these cells (49). To directly assess the impact of HS
379 sulfation on virus entry, we used several mutant cell lines deficient in HS sulfation
380 enzymes. All of these cells were defective in virus entry as assessed by IE1 protein
381 expression (Fig. 9.). Additional data from anti-3-*O*-S HS peptide confirmed the
382 significance of sulfation in HCMV infectivity. The GAG experiments used a fibroblast cell
383 culture system and a fibroblast tropic strain of HCMV (Towne), whereas MCMV
384 experiments used lung epithelial cells, thus providing the experimental data from
385 multiple cell types and two different viruses. While the GFP based assays provide a
386 surrogate for virus entry assays, the real impact of virus entry inhibitors would be a
387 reduction in viral titers at the end of infection since an entry inhibitor that only delays
388 virus entry would be of little translational value. Thus virus yield and titers were used a
389 measure of effectiveness of GAG inhibitors.

The enzymatic modification of HS chains is known to generate unique binding sites for viral ligands. For example, 3-*O*-sulfation modification in HS chain generates fusion receptor for HSV glycoprotein D (gD) promoting viral entry and spread (50). The 3-*O*-S HS is a product of enzymatic modification at C3 position of glucosamine residue, which is relatively rare in comparison to other HS modifications (Fig. 1B). Expression of Hs3st can make normally resistant Chinese hamster ovary (CHO-K1) cells susceptible to HSV-1 infection (51). Studies in clinically relevant primary human corneal fibroblasts have also shown 3-*O*-S HS as a primary attachment receptor for HSV entry (48). Interestingly, both HSV-1 and HSV-2 use HS as an attachment receptor but HSV-1 binds to distinct modification sites on HS that HSV-2 is unable to, which could explain some of the differences in cell tropism exhibited by these two viruses (52). For example, while N-sulfation and carboxyl groups are required for both HSV-1 and HSV-2 binding, only HSV-1 is able to bind the specific modification sites generated by 2-*O*, 6-*O,* and 3-*O*-sulfations (53). The *O*-desulfated heparins have little or no inhibitory effect on HSV-1 infection but inhibit HSV-2 infection. This susceptibility to *O*-desulfated heparins can be transferred to HSV-1 by recombinant transfer of the gene for glycoprotein C (gC-2) from HSV-2 (53). We reported earlier that 3-*O*-S HS are important for HCMV entry in human iris stromal (HIS) cells (43). The expression of Hs3st in HIS cells promoted HCMV internalization, while pretreatment of HIS cells with heparinase enzyme or treatment with anti-3-*O*-S HS (G2) peptide significantly reduced HCMV plaques/foci formation. In addition, co-culture of the HCMV-infected HIS cells with CHO-K1 cells expressing 3-*O*-S HS significantly enhanced cell fusion. A similar trend of enhanced fusion was observed

412 with cells expressing HCMV glycoproteins (gB, gO, and gH-gL) co-cultured with 3-*O*-S
413 HS cells. These results highlight the role of 3-*O*-S HS during HCMV entry.

414 Owing to their inherent structural features, certain sulfated glycans can exert
415 therapeutic effects against infections caused by pathogenic microorganisms. A study by
416 Pomin *et al.*, showed that administering sulfated glycans can disrupt the pathogen
417 protein-host glycosaminoglycan (GAG) complex formation causing impairment of
418 microbial binding onto host cells (54). Similarly, sulfated GAG, glycosphingolipids and
419 lectins have been shown to inhibit DENV entry (55). Heparan sulfate mimics, such as
420 suramin, pentosan polysulfate, and PI-88, SPGG (56, 57) have been reported to be
421 effective against multiple viruses including herpesviruses (4, 58, 59). The inhibitory
422 activity of HS mimics, including these compounds, is believed to be due to their
423 association with GAG binding sites of the putative receptor-binding domain on the viral
424 protein (4, 60). Thus, HS mimics can inhibit virus adsorption and entry.

425 Overall, the data from these studies indicate that *dp* of GAGs as well as specific
426 sulfation patterns govern HCMV infection of cells. These studies show the promise of
427 highly polymerized sulfated-HS as effective anti-CMV agents. Future studies will be
428 aimed at confirming the CMV glycoproteins that specifically bind to HS on cell surface
429 and their possible structural illustrations.

430

431 **Acknowledgments**

432 The research was supported by NASA (Award #80NSSC19K1603, PI: Tandon) and NIH
433 (Award R21HL131553, PI: L.W.). QL, JSS and LW acknowledge funding from the

National Institute of General Medical Sciences through the Research Resource for Integrated Glycotechnology (P41GM103390).

Author Contributions

RT, JSS, and LW designed the experiments; MHH, DM, LAF, RBP, QL, JSS, VT and RT performed the experiments and analyzed the data. RT and MHH wrote and edited the manuscript.

REFERENCES

1. Clausen TM, Sandoval DR, Spliid CB, Pihl J, Perrett HR, Painter CD, Narayanan A, Majowicz SA, Kwong EM, McVicar RN, Thacker BE, Glass CA, Yang Z, Torres JL, Golden GJ, Bartels PL, Porell RN, Garretson AF, Laubach L, Feldman J, Yin X, Pu Y, Hauser BM, Caradonna TM, Kellman BP, Martino C, Gordts P, Chanda SK, Schmidt AG, Godula K, Leibel SL, Jose J, Corbett KD, Ward AB, Carlin AF, Esko JD. 2020. SARS-CoV-2 Infection Depends on Cellular Heparan Sulfate and ACE2. Cell 183:1043-1057 e15.
2. Tandon R, Sharp JS, Zhang F, Pomin VH, Ashpole NM, Mitra D, McCandless MG, Jin W, Liu H, Sharma P, Linhardt RJ. 2021. Effective Inhibition of SARS-CoV-2 Entry by Heparin and Enoxaparin Derivatives. J Virol 95.
3. Barth H, Schäfer C, Adah MI, Zhang F, Linhardt RJ, Toyoda H, Kinoshita-Toyoda A, Toida T, van Kuppevelt TH, Depla E. 2003. Cellular binding of hepatitis C virus envelope glycoprotein E2 requires cell surface heparan sulfate. Journal of Biological Chemistry 278:41003-41012.
4. Chen Y, Maguire T, Hileman RE, Fromm JR, Esko JD, Linhardt RJ, Marks RM. 1997. Dengue virus infectivity depends on envelope protein binding to target cell heparan sulfate. Nature medicine 3:866.
5. Giroglou T, Florin L, Schäfer F, Streeck RE, Sapp M. 2001. Human papillomavirus infection requires cell surface heparan sulfate. Journal of virology 75:1565-1570.

462 6. Tyagi M, Rusnati M, Presta M, Giacca M. 2001. Internalization of HIV-1 tat
463 requires cell surface heparan sulfate proteoglycans. Journal of Biological
464 Chemistry 276:3254-3261.
465 7. Shukla D, Spear PG. 2001. Herpesviruses and heparan sulfate: an intimate
466 relationship in aid of viral entry. The Journal of clinical investigation 108:503-510.
467 8. Shukla D, Liu J, Blaiklock P, Shworak NW, Bai X, Esko JD, Cohen GH,
468 Eisenberg RJ, Rosenberg RD, Spear PG. 1999. A novel role for 3-O-sulfated
469 heparan sulfate in herpes simplex virus 1 entry. Cell 99:13-22.
470 9. Blanchard E, Belouzard S, Goueslain L, Wakita T, Dubuisson J, Wychowski C,
471 Rouillé Y. 2006. Hepatitis C virus entry depends on clathrin-mediated
472 endocytosis. Journal of virology 80:6964-6972.
473 10. Compton T, Feire A. 2007. Early events in human cytomegalovirus infection,
474 Human herpesviruses: biology, therapy, and immunoprophylaxis. Cambridge
475 University Press.
476 11. Ryckman BJ, Jarvis MA, Drummond DD, Nelson JA, Johnson DC. 2006. Human
477 cytomegalovirus entry into epithelial and endothelial cells depends on genes
478 UL128 to UL150 and occurs by endocytosis and low-pH fusion. Journal of
479 virology 80:710-722.
480 12. Podyma-Inoue KA, Moriwaki T, Rajapakshe AR, Terasawa K, Hara-Yokoyama
481 M. 2016. Characterization of heparan sulfate proteoglycan-positive recycling
482 endosomes isolated from glioma cells. Cancer Genomics-Proteomics 13:443-
483 452.

13. Park H, Kim M, Kim H-J, Lee Y, Seo Y, Pham CD, Lee J, Byun SJ, Kwon M-H. 2017. Heparan sulfate proteoglycans (HSPGs) and chondroitin sulfate proteoglycans (CSPGs) function as endocytic receptors for an internalizing anti-nucleic acid antibody. Scientific reports 7:14373.

14. Christianson HC, Belting M. 2014. Heparan sulfate proteoglycan as a cell-surface endocytosis receptor. Matrix Biology 35:51-55.

15. Sarrazin S, Lamanna WC, Esko JD. 2011. Heparan sulfate proteoglycans. Cold Spring Harbor perspectives in biology 3:a004952.

16. Varnum SM, Streblow DN, Monroe ME, Smith P, Auberry KJ, Paša-Tolić L, Wang D, Camp DG, Rodland K, Wiley S. 2004. Identification of proteins in human cytomegalovirus (HCMV) particles: the HCMV proteome. Journal of virology 78:10960-10966.

17. Spear PG, Shieh M-T, Herold BC, WuDunn D, Koshy TI. 1992. Heparan sulfate glycosaminoglycans as primary cell surface receptors for herpes simplex virus, p 341-353, Heparin and related polysaccharides. Springer.

18. Compton T, Nowlin DM, Cooper NR. 1993. Initiation of human cytomegalovirus infection requires initial interaction with cell surface heparan sulfate. Virology 193:834-841.

19. Laquerre S, Argnani R, Anderson DB, Zucchini S, Manservigi R, Glorioso JC. 1998. Heparan sulfate proteoglycan binding by herpes simplex virus type 1 glycoproteins B and C, which differ in their contributions to virus attachment, penetration, and cell-to-cell spread. Journal of virology 72:6119-6130.

20. Jacquet A, Haumont M, Chellun D, Massaer M, Tufaro F, Bollen A, Jacobs P. 1998. The varicella zoster virus glycoprotein B (gB) plays a role in virus binding to cell surface heparan sulfate proteoglycans. Virus research 53:197-207.

21. Wang X, Huong SM, Chiu ML, Raab-Traub N, Huang ES. 2003. Epidermal growth factor receptor is a cellular receptor for human cytomegalovirus. Nature 424:456-61.

22. Soroceanu L, Akhavan A, Cobbs CS. 2008. Platelet-derived growth factor-alpha receptor activation is required for human cytomegalovirus infection. Nature 455:391-5.

23. Feire AL, Roy RM, Manley K, Compton T. 2010. The glycoprotein B disintegrin-like domain binds beta 1 integrin to mediate cytomegalovirus entry. J Virol 84:10026-37.

24. Feire AL, Koss H, Compton T. 2004. Cellular integrins function as entry receptors for human cytomegalovirus via a highly conserved disintegrin-like domain. Proc Natl Acad Sci U S A 101:15470-5.

25. Boyle KA, Compton T. 1998. Receptor-binding properties of a soluble form of human cytomegalovirus glycoprotein B. Journal of virology 72:1826-1833.

26. Song BH, Lee GC, Moon MS, Cho YH, Lee CH. 2001. Human cytomegalovirus binding to heparan sulfate proteoglycans on the cell surface and/or entry stimulates the expression of human leukocyte antigen class I. Journal of General Virology 82:2405-2413.

27. Esko JD, Selleck SB. 2002. Order out of chaos: assembly of ligand binding sites in heparan sulfate. Annual review of biochemistry 71:435-471.

28. Multhaupt HA, Couchman JR. 2012. Heparan sulfate biosynthesis: methods for investigation of the heparanosome. Journal of Histochemistry & Cytochemistry 60:908-915.

29. Tiwari V, Liu J, Valyi-Nagy T, Shukla D. 2011. Anti-heparan sulfate peptides that block herpes simplex virus infection in vivo. J Biol Chem 286:25406-15.

30. Baldwin J, Maus E, Zanotti B, Volin MV, Tandon R, Shukla D, Tiwari V. 2015. A role for 3-O-sulfated heparan sulfate in promoting human cytomegalovirus infection in human iris cells. J Virol 89:5185-92.

31. Tiwari V, Tarbutton MS, Shukla D. 2015. Diversity of heparan sulfate and HSV entry: basic understanding and treatment strategies. Molecules 20:2707-27.

32. Ali MM, Karasneh GA, Jarding MJ, Tiwari V, Shukla D. 2012. A 3-O-sulfated heparan sulfate binding peptide preferentially targets herpes simplex virus 2-infected cells. J Virol 86:6434-43.

33. Wei Z, Lyon M, Gallagher JT. 2005. Distinct substrate specificities of bacterial heparinases against N-unsubstituted glucosamine residues in heparan sulfate. J Biol Chem 280:15742-8.

34. Kariya Y, Kyogashima M, Suzuki K, Isomura T, Sakamoto T, Horie K, Ishihara M, Takano R, Kamei K, Hara S. 2000. Preparation of completely 6-O-desulfated heparin and its ability to enhance activity of basic fibroblast growth factor. J Biol Chem 275:25949-58.

35. Qiu H, Shi S, Yue J, Xin M, Nairn AV, Lin L, Liu X, Li G, Archer-Hartmann SA, Dela Rosa M, Galizzi M, Wang S, Zhang F, Azadi P, van Kuppevelt TH, Cardoso WV, Kimata K, Ai X, Moremen KW, Esko JD, Linhardt RJ, Wang L. 2018. A

552 mutant-cell library for systematic analysis of heparan sulfate structure-function
553 relationships. Nat Methods 15:889-899.
554 36. Zurbach KA, Moghbeli T, Snyder CM. 2014. Resolving the titer of murine
555 cytomegalovirus by plaque assay using the M2-10B4 cell line and a low viscosity
556 overlay. Virol J 11:71.
557 37. Alam SM, Aussedat B, Vohra Y, Meyerhoff RR, Cale EM, Walkowicz WE,
558 Radakovich NA, Anasti K, Armand L, Parks R, Sutherland L, Scearce R, Joyce
559 MG, Pancera M, Druz A, Georgiev IS, Von Holle T, Eaton A, Fox C, Reed SG,
560 Louder M, Bailer RT, Morris L, Abdool-Karim SS, Cohen M, Liao HX, Montefiori
561 DC, Park PK, Fernandez-Tejada A, Wiehe K, Santra S, Kepler TB, Saunders KO,
562 Sodroski J, Kwong PD, Mascola JR, Bonsignori M, Moody MA, Danishefsky S,
563 Haynes BF. 2017. Mimicry of an HIV broadly neutralizing antibody epitope with a
564 synthetic glycopeptide. Sci Transl Med 9.
565 38. Reddehase MJ, Lemmermann NAW. 2018. Mouse Model of Cytomegalovirus
566 Disease and Immunotherapy in the Immunocompromised Host: Predictions for
567 Medical Translation that Survived the "Test of Time". Viruses 10.
568 39. Brune W, Hengel H, Koszinowski UH. 2001. A mouse model for cytomegalovirus
569 infection. Curr Protoc Immunol Chapter 19:Unit 19 7.
570 40. Cekinovic D, Lisnic VJ, Jonjic S. 2014. Rodent models of congenital
571 cytomegalovirus infection. Methods Mol Biol 1119:289-310.
572 41. Sauer B. 1987. Functional expression of the cre-lox site-specific recombination
573 system in the yeast Saccharomyces cerevisiae. Mol Cell Biol 7:2087-96.

574 42. Zhang F, Wen Y, Guo X. 2014. CRISPR/Cas9 for genome editing: progress,
575 implications and challenges. Hum Mol Genet 23:R40-6.
576 43. Baldwin J, Maus E, Zanotti B, Volin MV, Tandon R, Shukla D, Tiwari V. 2015. A
577 role for 3-O-sulfated heparan sulfate in promoting human cytomegalovirus
578 infection in human iris cells. Journal of virology 89:5185-5192.
579 44. Oduro JD, Uecker R, Hagemeier C, Wiebusch L. 2012. Inhibition of human
580 cytomegalovirus immediate-early gene expression by cyclin A2-dependent
581 kinase activity. J Virol 86:9369-83.
582 45. Adamson CS, Nevels MM. 2020. Bright and Early: Inhibiting Human
583 Cytomegalovirus by Targeting Major Immediate-Early Gene Expression or
584 Protein Function. Viruses 12.
585 46. Archer MA, Brechtel TM, Davis LE, Parmar RC, Hasan MH, Tandon R. 2017.
586 Inhibition of endocytic pathways impacts cytomegalovirus maturation. Sci Rep
587 7:46069.
588 47. Dunn W, Chou C, Li H, Hai R, Patterson D, Stolc V, Zhu H, Liu F. 2003.
589 Functional profiling of a human cytomegalovirus genome. Proc Natl Acad Sci U S
590 A 100:14223-8.
591 48. Tiwari V, Clement C, Xu D, Valyi-Nagy T, Yue BY, Liu J, Shukla D. 2006. Role
592 for 3-O-sulfated heparan sulfate as the receptor for herpes simplex virus type 1
593 entry into primary human corneal fibroblasts. Journal of virology 80:8970-8980.
594 49. Qiu H, Shi S, Yue J, Xin M, Nairn AV, Lin L, Liu X, Li G, Archer-Hartmann SA,
595 Dela Rosa M, Galizzi M, Wang S, Zhang F, Azadi P, van Kuppevelt TH, Cardoso
596 WV, Kimata K, Ai X, Moremen KW, Esko JD, Linhardt RJ, Wang L. 2018. A

mutant-cell library for systematic analysis of heparan sulfate structure–function relationships. Nature Methods doi:10.1038/s41592-018-0189-6.

50. Tiwari V, Tarbutton M, Shukla D. 2015. Diversity of heparan sulfate and HSV entry: basic understanding and treatment strategies. Molecules 20:2707-2727.

51. Tiwari V, O'Donnell C, Copeland RJ, Scarlett T, Liu J, Shukla D. 2007. Soluble 3-O-sulfated heparan sulfate can trigger herpes simplex virus type 1 entry into resistant Chinese hamster ovary (CHO-K1) cells. Journal of General Virology 88:1075-1079.

52. O'Donnell CD, Kovacs M, Akhtar J, Valyi-Nagy T, Shukla D. 2010. Expanding the role of 3-O sulfated heparan sulfate in herpes simplex virus type-1 entry. Virology 397:389-398.

53. Herold BC, Gerber SI, Belval BJ, Siston AM, Shulman N. 1996. Differences in the susceptibility of herpes simplex virus types 1 and 2 to modified heparin compounds suggest serotype differences in viral entry. Journal of virology 70:3461-3469.

54. Pomin VH. 2017. Antimicrobial Sulfated Glycans: Structure and Function. Curr Top Med Chem 17:319-330.

55. Hidari KI, Abe T, Suzuki T. 2013. Carbohydrate-related inhibitors of dengue virus entry. Viruses 5:605-18.

56. Gangji RN, Sankaranarayanan NV, Elste J, Al-Horani RA, Afosah DK, Joshi R, Tiwari V, Desai UR. 2018. Inhibition of Herpes Simplex Virus-1 Entry into Human Cells by Nonsaccharide Glycosaminoglycan Mimetics. ACS Med Chem Lett 9:797-802.

620 57. Majmudar H, Hao M, Sankaranarayanan NV, Zanotti B, Volin MV, Desai UR,
621 Tiwari V. 2019. A synthetic glycosaminoglycan mimetic blocks HSV-1 infection in
622 human iris stromal cells. Antiviral Res 161:154-162.
623 58. Lee E, Pavy M, Young N, Freeman C, Lobigs M. 2006. Antiviral effect of the
624 heparan sulfate mimetic, PI-88, against dengue and encephalitic flaviviruses.
625 Antiviral Res 69:31-8.
626 59. Marks RM, Lu H, Sundaresan R, Toida T, Suzuki A, Imanari T, Hernaiz MJ,
627 Linhardt RJ. 2001. Probing the interaction of dengue virus envelope protein with
628 heparin: assessment of glycosaminoglycan-derived inhibitors. J Med Chem
629 44:2178-87.
630 60. Modis Y, Ogata S, Clements D, Harrison SC. 2003. A ligand-binding pocket in
631 the dengue virus envelope glycoprotein. Proc Natl Acad Sci U S A 100:6986-91.
632 61. Poulain FE, Yost HJ. 2015. Heparan sulfate proteoglycans: a sugar code for
633 vertebrate development? Development 142:3456-67.

FIGURE LEGENDS

Figure 1. Structural features of heparan sulfate. (A) HS is a linear polysaccharide composed of repeating uronic acid [D-glucuronic acid (GlcA) or L-iduronic acid (IdoA)] and D-glucosamine (GlcN) disaccharide subunits. Synthesized chain of HS represents assembly of the tetrasaccharide linker region (GlcA-Gal-Gal- Xyl) at reducing end on serine residues of the protein core followed by the addition of alternating GlcA and GlcNAc residues. The chain extension is also accompanied by a series of modifications, which include 6-*O*, 3-*O* sulfations on GlcN and the 2-*O* sulfation on GlcA. The arrow shows the 3-*O* position of the GlcN where sulfation is important for herpesvirus binding (15, 50).

(B) Heparan sulfate chains are initially synthesized as repeating disaccharide units of N-acetylated glucosamine and glucuronic acid. HS can then be modified by a series of enzymatic reactions, including N-deacetylation and N-sulfation of N-acetylated glucosamine converting it to N-sulfo-glucosamine, C5 epimerization of glucuronic acid to iduronic acid, and O-sulfation at the 2-OH, 6-OH, and 3-OH positions. Among sulfations, first is 2-*O*-sulfation of iduronic acid and glucuronic acid, followed by 6-*O*-sulfation of N-acetylated glucosamine and N-sulfo-glucosamine units, and finally 3-*O*-sulfation of glucosamine residues (52, 61).

Fig. 1A.

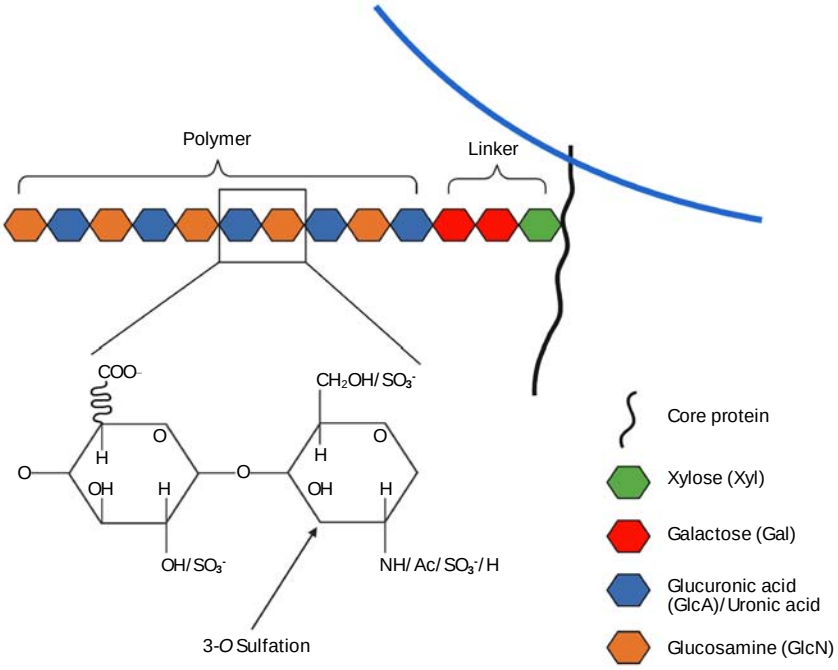

Fig. 1B

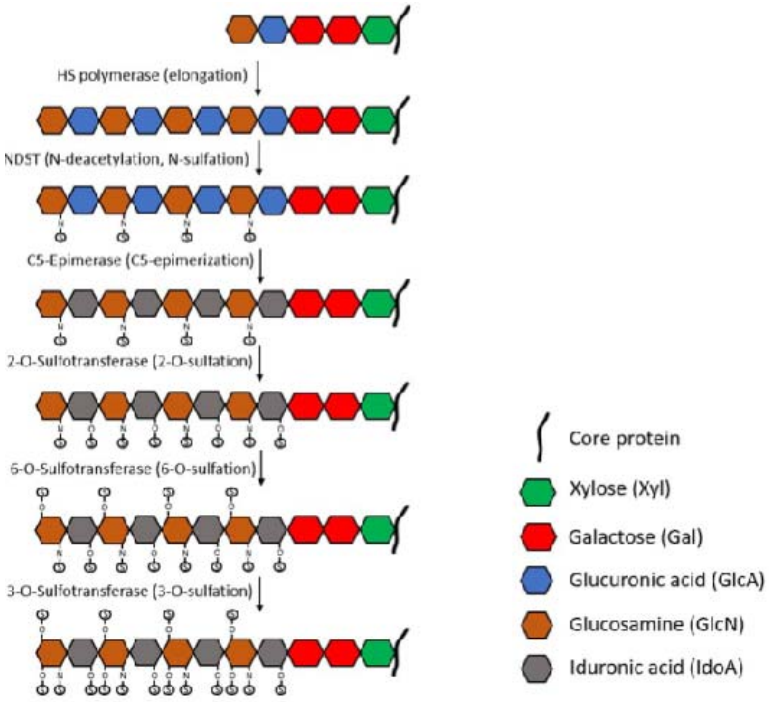

Figure 2. Binding of purified extracellular CMV virions on a custom designed glycosaminoglycan glycoarray. Relative fluorescence units (RFU), which are directly proportional to the amount of virus binding, are plotted on the Y-axis in the graph. Ligand descriptions and chain structures are provided in Table 1. Six replicates for each GAG were used in the assay. NC: Negative control (print buffer), PC1: positive control (Biotinylated Glycan), PC2: human IgG (0.1 mg/ml), PC3: mouse IgG (0.1 mg/ml), PC4: rabbit IgG (0.1 mg/ml), *dp*: degree of polymerization, triangles at the bottom of the graph represent an increasing degree of polymerization of GAGs from left to right. The virus preparation does not contain streptavidin label and thus PC1 serves as a negative rather than a positive control.

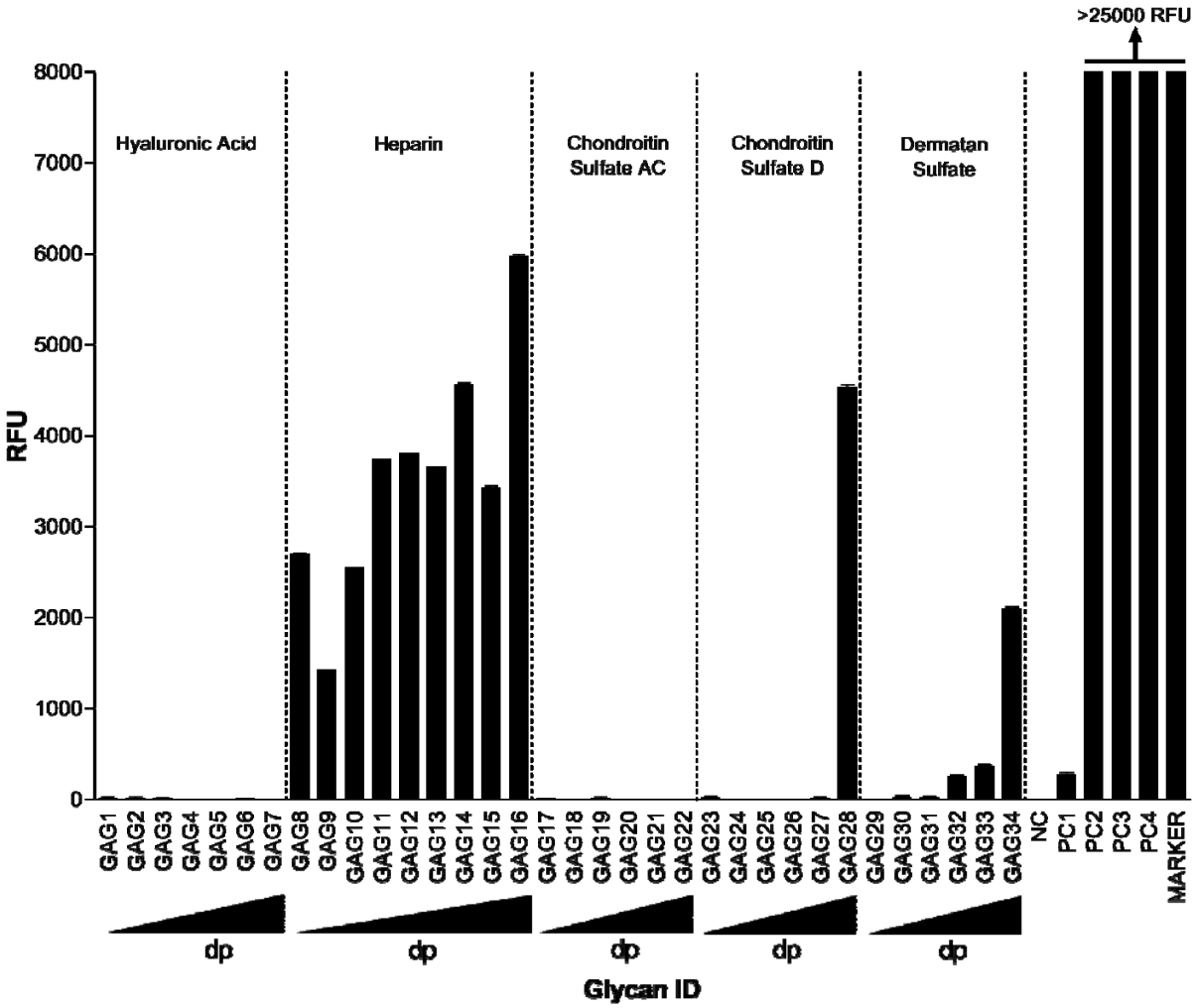

Figure 3. Binding of purified extracellular CMV on a custom designed heparan sulfate glycoarray. Relative fluorescence units (RFU), which are directly proportional to the amount of virus binding, are plotted on the Y-axis in the graph. Ligand descriptions and chain structures are provided in Table 2. Six replicates for each ligand were used. NC: negative control (print buffer) PC1: positive control (biotinylated glycan), PC2: human IgG (0.1 mg/ml), PC3: mouse IgG (0.1 mg/ml), PC4: rabbit IgG (0.1 mg/ml). The virus preparation does not contain streptavidin label and thus PC1 serves as a negative rather than a positive control.

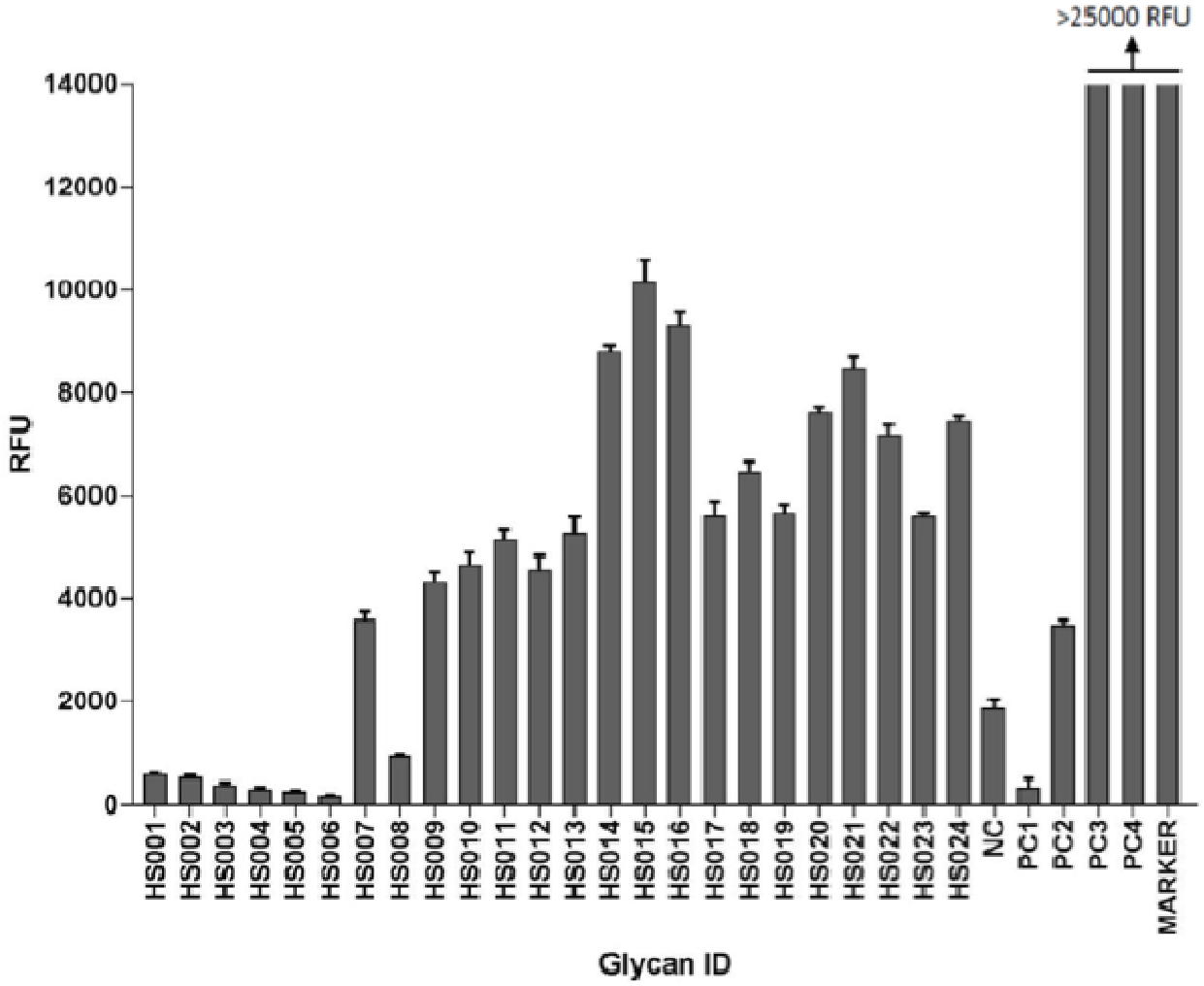

Figure 4. Inhibition of HCMV growth by glycosaminoglycan derivatives. Primary human foreskin fibroblasts (HFF) grown in 96 well plate were pretreated for one hour with 10 µM of 1) 6-*O*-desulfated Arixtra, 2) Unmodified Arixtra, 3) Heparin sodium salt from porcine intestinal mucosa (PIHSS), 4) Enoxaparin, or series of heparin oligosaccharide from enoxaparin: 5) *dp2*, 6) *dp4*, 7) *dp6*, 8) *dp8*, 9) *dp10*, 10) *dp12*, 11) *dp14*, 12) *dp16*, 13) *dp18*, 14) dp20 15) > *dp20* or control (dH2O). Cells were infected with GFP tagged HCMV (Towne strain) virus at an MOI of 3.0 in the presence of the test glycosaminoglycans. At 5 days post-infection, cells were fixed and number of foci (GFP) was counted under an epifluorescent microscope. Percent of viral GFP was calculated compared to virus only infected control (100% GFP expression). Results are representative of three independent replicates. Standard error of mean was plotted as error bars.

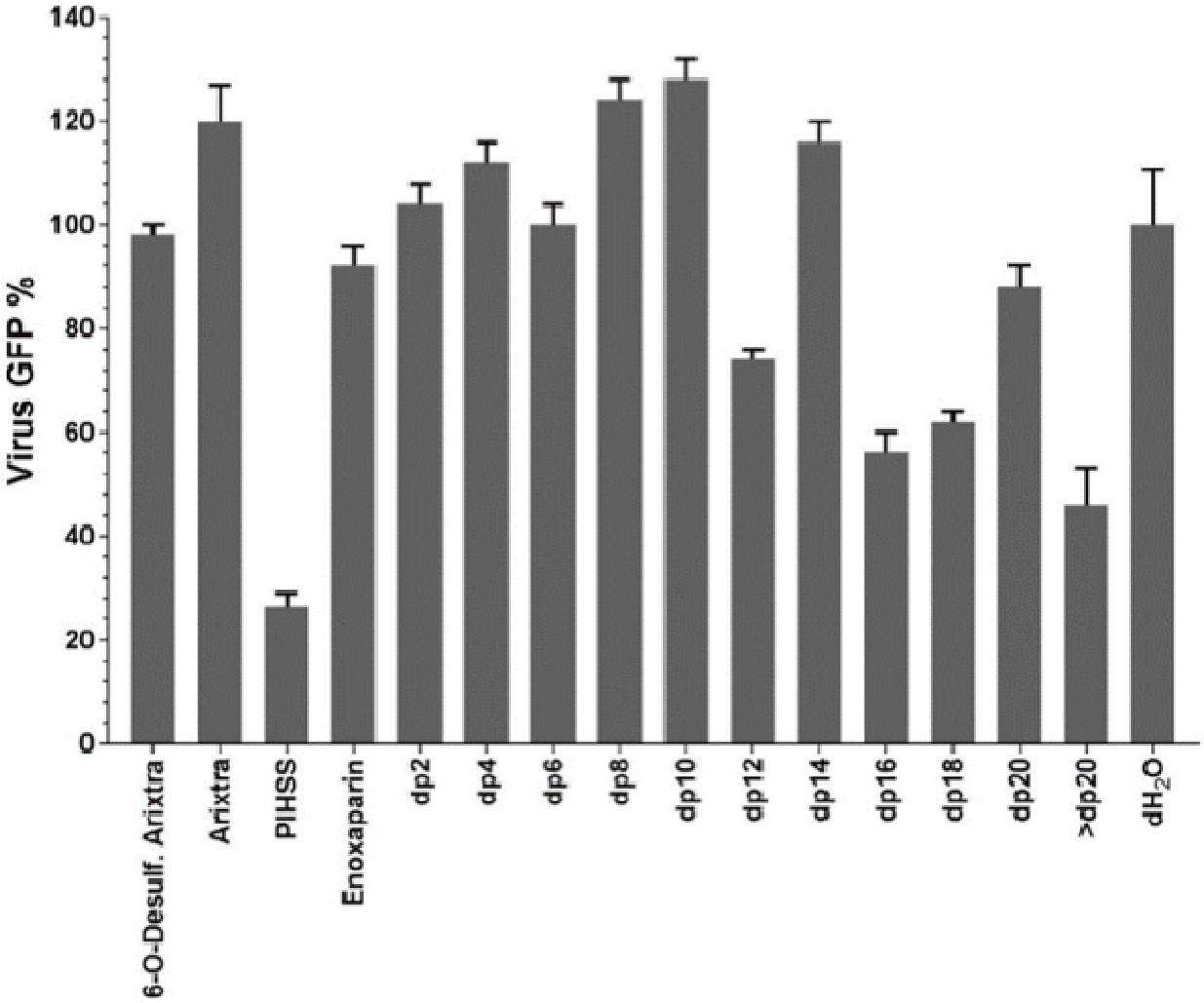

Figure 5. Effect of glycosaminoglycan derivatives at 10 μM concentration on HCMV growth. (A) Primary human foreskin fibroblasts (HFF) were pretreated for one hour with 10 μM of 1) 6-*O*-desulfated Arixtra, 2) Regular Arixtra, 3) Heparin sodium salt from porcine intestinal mucosa (PIHSS), 4) Enoxaparin, or series of heparin oligosaccharide from enoxaparin: 5) *dp2*, 6) *dp4*, 7) *dp6*, 8) *dp8*, 9) *dp10*, 10) *dp12*, 11) *dp14*, 12) *dp16*, 13) *dp18*, 14) *dp20* 15) > *dp20* or control (dH2O). Cells were infected with HCMV (Towne strain) virus at an MOI of 3.0 in the presence of test glycosaminoglycans. Cells and media were harvested at 5 days post-infection and titered for HCMV plaque forming units (pfu) on fresh fibroblasts in tissue culture dishes. Individual samples (3 replicates each) were quantified and displayed as total pfu/ml on Y-axis. (B) Virus titer is plotted (Y-axis) against degree of polymerization (X-axis). Data points ahead of the broken line is for a mixture of GAGs (*dp*>20). Results are representative of three independent replicates. Standard error of mean was plotted as error bars.

A.

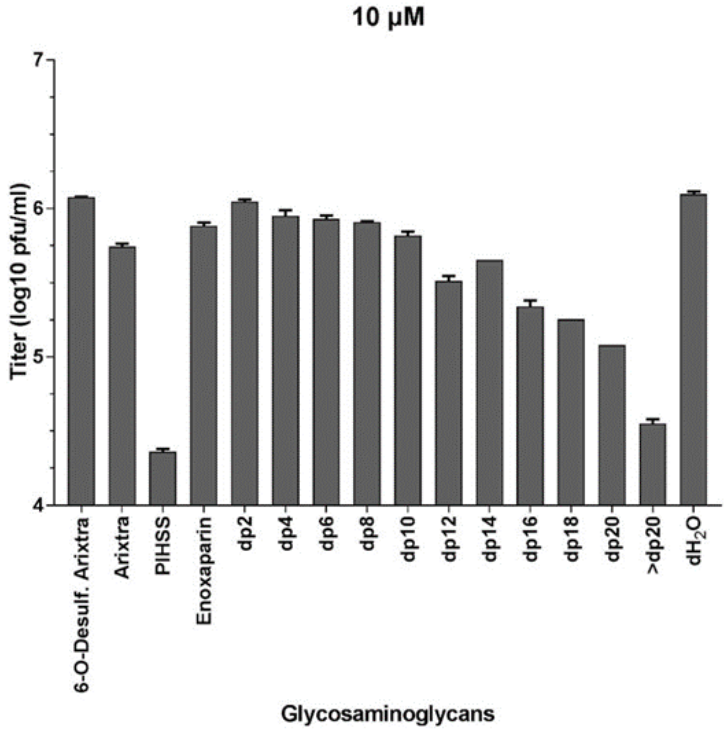

B.

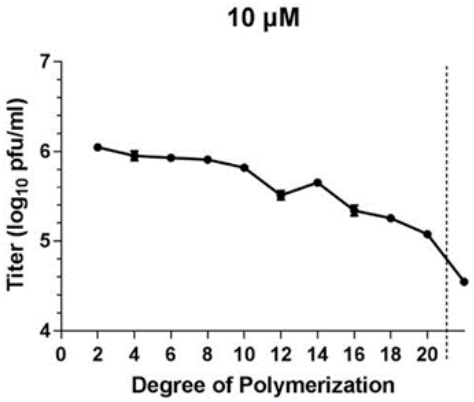

Figure 6. Effect of glycosaminoglycan derivatives at 0.05 g/L concentration on HCMV growth. (A) Primary human foreskin fibroblasts (HFF) were pretreated for one hour with 0.05 g/L of 1) 6-*O*-desulfated Arixtra, 2) Regular Arixtra, 3) Heparin sodium salt from porcine intestinal mucosa (PIHSS), 4) Enoxaparin, or series of heparin oligosaccharide from enoxaparin: 5) *dp2*, 6) *dp4*, 7) *dp6*, 8) *dp8*, 9) *dp10*, 10) *dp12*, 11) *dp14*, 12) *dp16*, 13) *dp18*, 14) *dp20* 15) > *dp20* or control (dH2O). Cells were infected with HCMV (Towne strain) virus at an MOI of 3.0 in the presence of test glycosaminoglycans. Cells and media were harvested at 5 days post-infection and titered for HCMV plaque forming units (pfu) on fresh fibroblasts in tissue culture dishes. Individual samples (3 replicates each) were quantified and displayed as total pfu/ml on Y-axis. (B) Virus titer is plotted (Y-axis) against degree of polymerization (X-axis). Data points ahead of the broken line is for a mixture of GAGs (*dp*>20). Results are representative of three independent replicates. Standard error of mean was plotted as error bars.

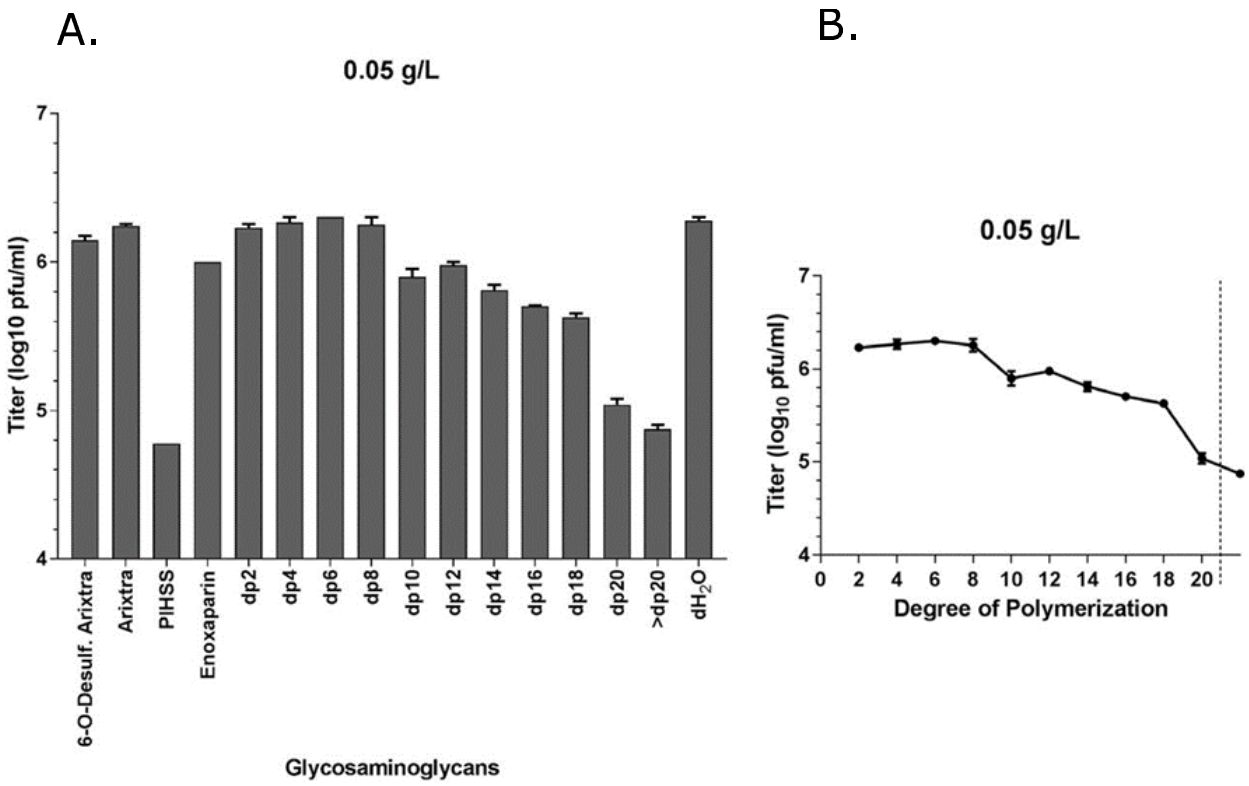

Figure 7. Effect of GAG treatment on cell viability of HFF cells. Primary HFF were pretreated for one hour with 10 µM of 1) 6-*O*-desulfated Arixtra, 2) Regular Arixtra, 3) Heparin sodium salt from porcine intestinal mucosa (PIHSS), 4) Enoxaparin, or series of heparin oligosaccharide from enoxaparin: 5) *dp2*, 6) *dp4*, 7) *dp6*, 8) *dp8*, 9) *dp10*, 10) *dp12*, 11) *dp14*, 12) *dp16*, 13) *dp18*, 14) *dp20*, 15) > *dp20* or control (dH2O). Cells were either mock infected (A) or infected with HCMV (Towne strain) virus at an MOI of 3.0 (B) in the presence of test glycosaminoglycans. Cells were harvested at 5 days post-infection and cell viability was assessed using Trypan Blue exclusion assay. Results are representative of three independent replicates. Standard error of mean was plotted as error bars.

A.

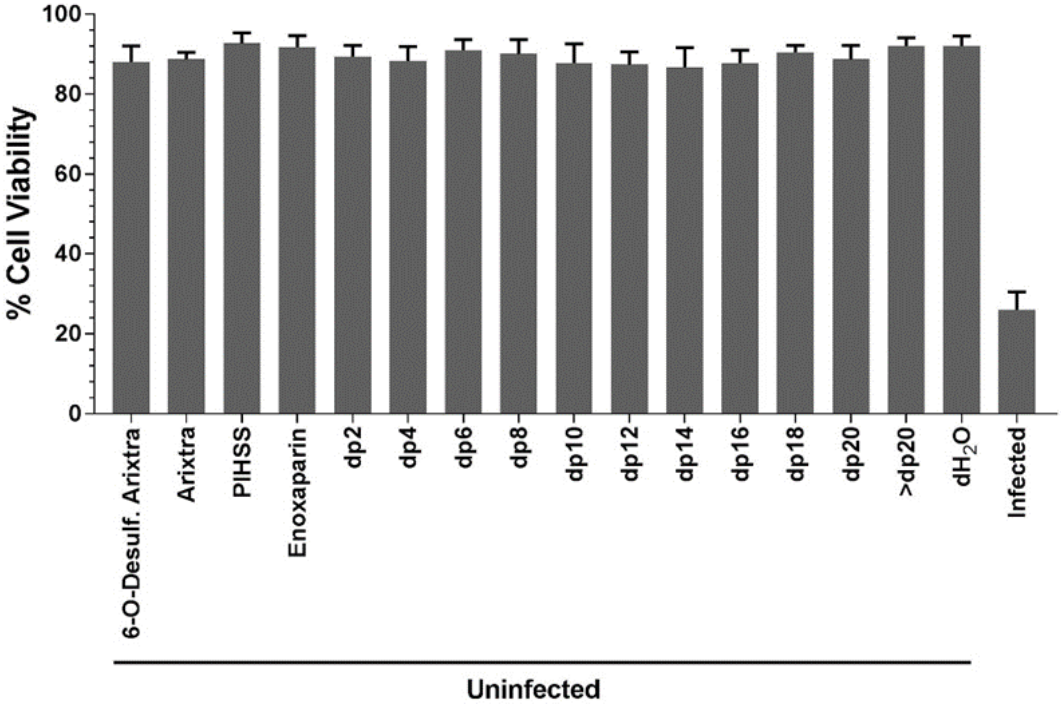

B.

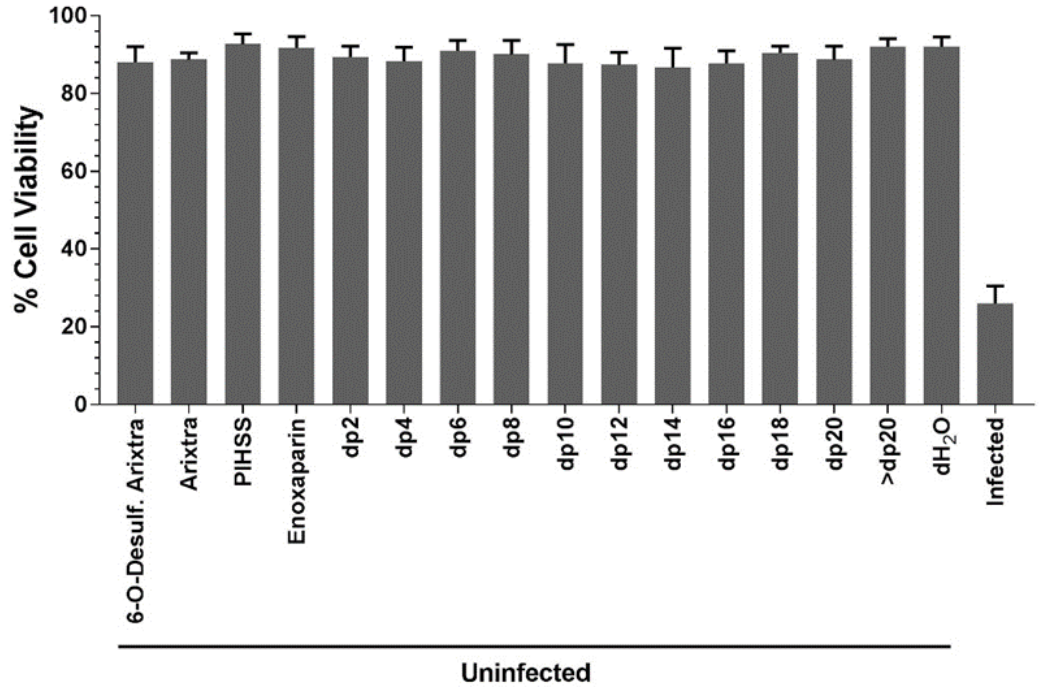

Figure 8. Mouse CMV replication in sulfotransferase knockout cell lines. Cells were grown to 90% confluency and infected with wild-type MCMV (strain K181) at low (0.01, A, B) and high (3.0, C, D) MOI. Cells and the medium were harvested at 3- and 5-days post-infection, sonicated to release the virus and diluted for plating on to wild-type MEF in tissue culture dishes in order to enumerate total MCMV pfu/ml. Results are representative of three independent replicates. A student's t-test was conducted in Graphpad Prism comparing the means of different groups. A p-value <0.05 was considered significant. Standard error of mean was plotted as error bars. An asterisk (*) indicates significant inhibition compared to wild-type. Hs3st1 and Hs3st4: Glucosaminyl 3-*O*-sulfotransferase 1 and 4, respectively. WT: wild type; KO: knockout.

MOI 0.01

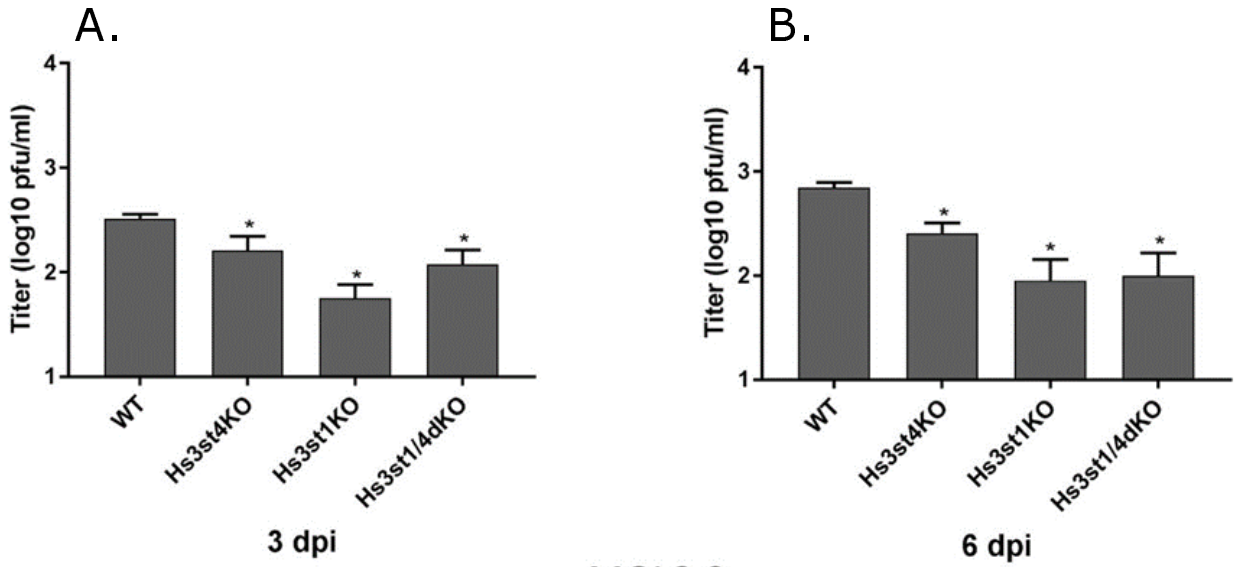

MOI 3.0

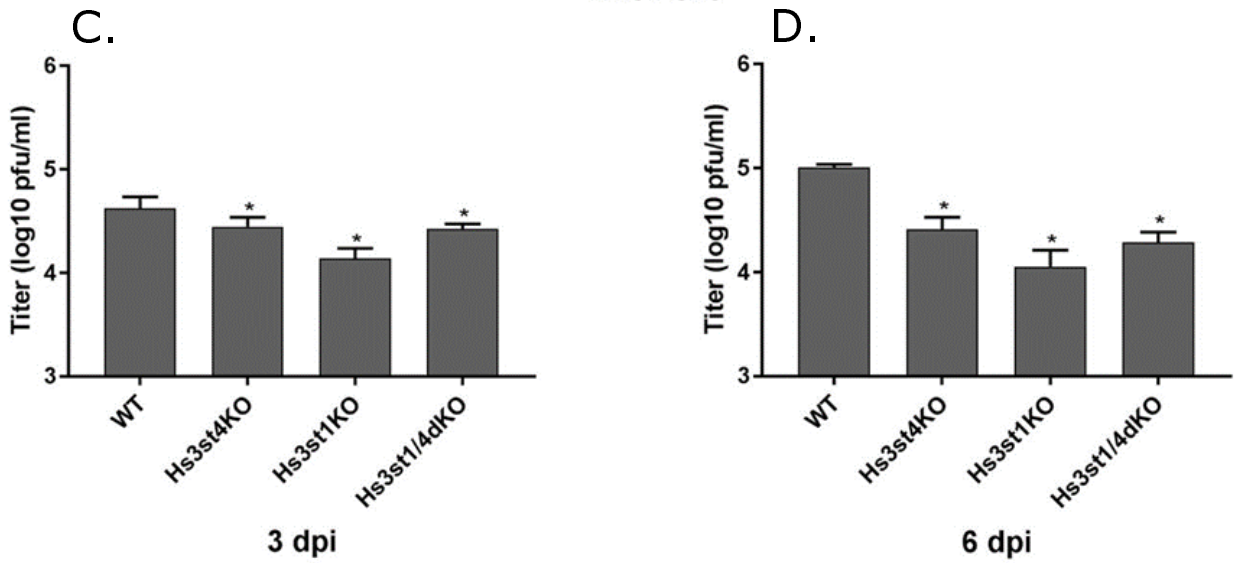

Figure 9. Mouse CMV entry in sulfotransferase knockout cell lines. A. Cells were grown to 90% confluency and infected with wild-type MCMV (strain K181) at an MOI of 3.0. Cells were harvested at 2 hours post-infection, and whole cell lysates were loaded on a polyacrylamide gel for blotting. The blots were probed with anti IE1 antibody. Beta-actin was used as a loading control. B. Bands from two independent experiments were quantified by densitometry and means were plotted. Standard error of mean was plotted as error bars. Hs6st1 and Hs6st4: Glucosaminyl 6-*O*-sulfotransferase 1 and 4, respectively. Hs3st1 and Hs3st4: Glucosaminyl 3-*O*-sulfotransferase 1 and 4, respectively. WT: wild type; dko: double knockout.

A.

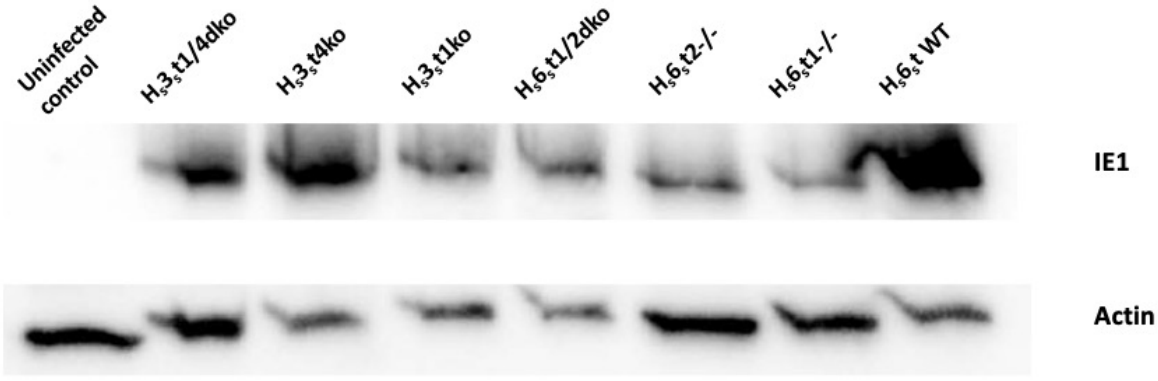

B.

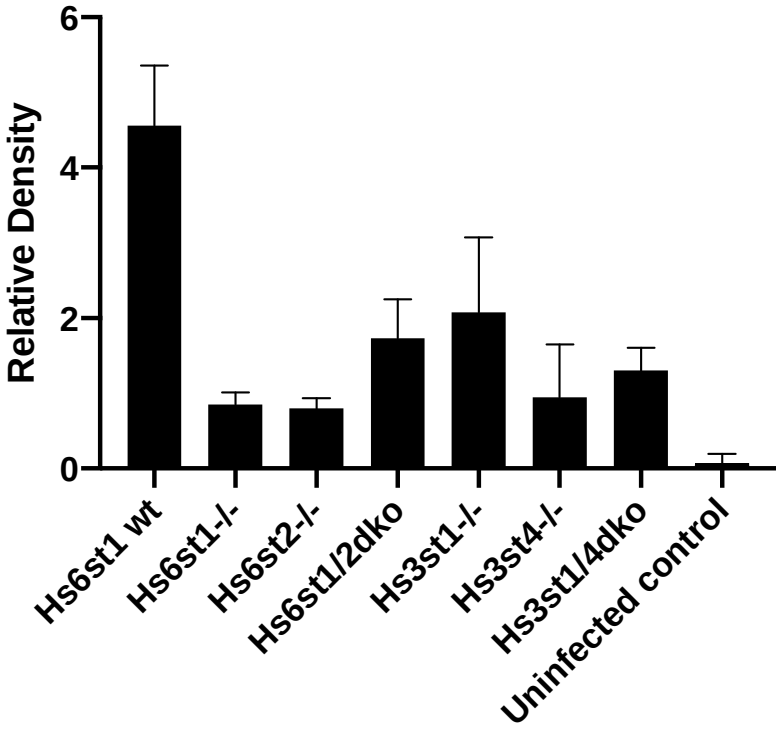

Figure 10. Effect of anti-3-O-S HS peptide on CMV infectivity in HFF cells. HFF cells were pre-treated with wild-type HS peptide, anti 3-OS HS peptide for 4 hrs. The mock treated cells were used as a positive control. The cells were infected with β-galactosidase expressing CMV for 9 days. β-Galactosidase assay was performed using X-gal (Sigma). The effect of entry-blocking activity of peptide was examined by counting number of foci. Results are representative of three independent experiments. A student's t-test was conducted in Graphpad Prism comparing the means of each group. A p value <0.05 was considered significant. Standard error of mean was plotted as error bars. Both anti-HS and anti 3-O-S HS showed significant inhibition compared to mock.